Validation of joint input-state estimation for force identification and response estimation in structural dynamics

K. Maes[1], K. Van Nimmen[1,2], E. Lourens[3], A. Rezayat[4], P. Guillaume[4], G. De Roeck[1], G. Lombaert[1]

[1] KU Leuven, Department of Civil Engineering, Leuven, Belgium, kristof.maes@kuleuven.be
[2] KU Leuven, Department of Civil Engineering, Technology Cluster Construction, Ghent, Belgium
[3] Delft University of Technology, Faculty of Civil Engineering and Geosciences, Delft, The Netherlands
[4] Vrije Universiteit Brussel, Department of Mechanical Engineering, Brussels, Belgium

Keywords: force identification, response estimation, joint input-state estimation, data fusion, structural health monitoring

Abstract

This paper presents a validation of a recently developed joint input-state estimation algorithm for force identification and response estimation in structural dynamics, using data obtained from in situ experiments on a footbridge. First, the algorithm is used to identify two impact forces applied to the bridge deck. Next, the algorithm is used to extrapolate measured accelerations due to wind loading to unmeasured locations in the structure. The dynamic model of the footbridge used in the system inversion is obtained from a detailed finite element model, that is calibrated using a set of experimental modal characteristics. The quality of the estimated forces and accelerations is assessed by comparison with the corresponding measured quantities. In both cases, a very good overall agreement is obtained.

1. INTRODUCTION

The knowledge of the loads applied to structures and the corresponding system response is very important for many engineering applications. Often, however, the dynamic forces acting on a structure cannot be obtained by direct measurements, for example wind loads on tall buildings or dynamic vehicle loads on bridges. In addition, the response of a structure cannot be measured at all physical locations, due to practical and economical considerations. System inversion techniques allow combining available vibration data from a limited number of sensors with the information obtained from a dynamic model of the structure, hereby estimating the forces acting to the structure and the response at unmeasured locations.

Several force identification algorithms have been proposed in the literature [1–3]. Additionally, several state estimation algorithms have been proposed, for linear as well as for non-linear systems [4]. A common approach in state estimation consists of modeling the system input as zero mean Gaussian white noise, where a Bayesian framework is applied for state estimation [5]. In order to overcome the assumption of white noise system input, joint input-state estimation algorithms have been developed, that combine both input and state estimation, e.g. [6, 7]. Gillijns and De Moor [8] have proposed an algorithm where the input estimation is performed prior to the state estimation step. The algorithm was introduced in structural dynamics by Lourens et al. [9], and further extended in [10]. A verification of the algorithm for force identification is presented in [11]. The algorithm was also applied for the estimation of strains in the tower of an offshore monopile wind turbine in [12], where a comparison is made to the classical Kalman filter [13] and a state-of-the-art modal expansion algorithm [14].

This paper presents a full-scale verification of the joint input-state estimation algorithm introduced in [10], using data obtained from in situ measurements on a footbridge. The algorithm is first applied for the identification of two impact forces applied to the bridge deck [11]. Next, the algorithm is applied for

the extrapolation of measured accelerations to other locations on the bridge deck. The estimated forces and accelerations are verified by comparing them to the actual measured quantities.

The outline of the paper is as follows. Section 2. gives a brief overview of the joint input-state estimation algorithm. Next, section 3. shows the measurement setup on the footbridge. Section 4. presents the dynamic system model that is used in the system inversion. Sections 5. and 6. show the results of the force identification and response estimation, respectively. Finally, section 7. concludes the paper.

2. MATHEMATICAL FORMULATION

This section gives a brief summary of the joint input-state estimation algorithm introduced in [10] and its application for force identification and response estimation.

Consider the following discrete-time linear combined deterministic-stochastic state-space description of a system:

$$\mathbf{x}_{[k+1]} = \mathbf{A}\mathbf{x}_{[k]} + \mathbf{B}\mathbf{p}_{[k]} + \mathbf{w}_{[k]} \tag{1}$$

$$\mathbf{d}_{[k]} = \mathbf{G}\mathbf{x}_{[k]} + \mathbf{J}\mathbf{p}_{[k]} + \mathbf{v}_{[k]} \tag{2}$$

where $\mathbf{x}_{[k]} \in \mathbb{R}^{n_\mathrm{s}}$ is the state vector, $\mathbf{d}_{[k]} \in \mathbb{R}^{n_\mathrm{d}}$ is the output vector, assumed to be measured, and $\mathbf{p}_{[k]} \in \mathbb{R}^{n_\mathrm{p}}$ is the unknown input vector, with n_s the number of system states, n_d the number of outputs, and n_p the number of inputs. The system matrices $\mathbf{A}$, $\mathbf{B}$, $\mathbf{G}$, and $\mathbf{J}$ are assumed known. Throughout the derivation of the algorithm, it is assumed that the sensor network meets the conditions for instantaneous system inversion derived in [15].

The process noise vector $\mathbf{w}_{[k]} \in \mathbb{R}^{n_\mathrm{s}}$ and measurement noise vector $\mathbf{v}_{[k]} \in \mathbb{R}^{n_\mathrm{d}}$ both account for unknown excitation sources and modeling errors. The measurement noise vector $\mathbf{v}_{[k]}$ also accounts for measurement errors [10]. The noise processes $\mathbf{w}_{[k]}$ and $\mathbf{v}_{[k]}$ are assumed to be zero mean and white, with known covariance matrices $\mathbf{Q}$, $\mathbf{R}$, and $\mathbf{S}$, defined by:

$$\mathbb{E}\left\{ \begin{pmatrix} \mathbf{w}_{[k]} \\ \mathbf{v}_{[k]} \end{pmatrix} \begin{pmatrix} \mathbf{w}_{[l]}^\mathrm{T} & \mathbf{v}_{[l]}^\mathrm{T} \end{pmatrix} \right\} = \begin{bmatrix} \mathbf{Q} & \mathbf{S} \\ \mathbf{S}^\mathrm{T} & \mathbf{R} \end{bmatrix} \delta_{[k-l]} \tag{3}$$

with $\mathbf{R} > 0$, $\begin{bmatrix} \mathbf{Q} & \mathbf{S} \\ \mathbf{S}^\mathrm{T} & \mathbf{R} \end{bmatrix} \geq 0$, and $\delta_{[k]} = 1$ for $k = 0$ and 0 otherwise. $\mathbb{E}\{\cdot\}$ is the expectation operator. Finally, it is assumed that an unbiased estimate $\hat{\mathbf{x}}_{[0|-1]}$ of the initial state is available, with error covariance matrix $\mathbf{P}_{\mathrm{x}[0|-1]}$ (i.e. $\mathbb{E}\left\{\mathbf{x}_{[0]} - \hat{\mathbf{x}}_{[0|-1]}\right\} = 0$, $\mathbf{P}_{\mathrm{x}[0|-1]} = \mathbb{E}\left\{(\mathbf{x}_{[0]} - \hat{\mathbf{x}}_{[0|-1]})(\mathbf{x}_{[0]} - \hat{\mathbf{x}}_{[0|-1]})^\mathrm{T}\right\}$). The estimate $\hat{\mathbf{x}}_{[0|-1]}$ is assumed independent on the noise processes $\mathbf{w}_{[k]}$ and $\mathbf{v}_{[k]}$ for all k.

The joint input-state estimation algorithm consists of a three-step recursive filter [8, 10]:

$$\hat{\mathbf{p}}_{[k|k]} = \mathbf{M}_{[k]} \left(\mathbf{d}_{[k]} - \mathbf{G}\hat{\mathbf{x}}_{[k|k-1]}\right) \tag{4}$$

$$\hat{\mathbf{x}}_{[k|k]} = \hat{\mathbf{x}}_{[k|k-1]} + \mathbf{K}_{[k]} \left(\mathbf{d}_{[k]} - \mathbf{G}\hat{\mathbf{x}}_{[k|k-1]} - \mathbf{J}\hat{\mathbf{p}}_{[k|k]}\right) \tag{5}$$

$$\hat{\mathbf{x}}_{[k+1|k]} = \mathbf{A}\hat{\mathbf{x}}_{[k|k]} + \mathbf{B}\hat{\mathbf{p}}_{[k|k]} \tag{6}$$

The first step in equation (4), referred to as the "input estimation step", yields a filtered estimate of the unknown input vector $\mathbf{p}_{[k]}$, given the measured output $\mathbf{d}_{[k]}$ up to time step k. The second step in equation (5), referred to as the "measurement update", yields a filtered estimate of the state vector $\mathbf{x}_{[k]}$. The third step in equation (6), referred to as the "time update", yields a one step ahead prediction of the state vector $\mathbf{x}_{[k+1]}$. The gain matrices $\mathbf{M}_{[k]} \in \mathbb{R}^{n_\mathrm{p} \times n_\mathrm{d}}$ and $\mathbf{K}_{[k]} \in \mathbb{R}^{n_\mathrm{s} \times n_\mathrm{d}}$ are determined such that both the input estimates $\hat{\mathbf{p}}_{[k|k]}$ and the state estimates $\hat{\mathbf{x}}_{[k|k]}$ are minimum variance and unbiased (MVU) [8], i.e. the uncertainty on the force and state estimates is minimized, and the error on the estimated forces $\hat{\mathbf{p}}_{[k|k]}$ and states $\hat{\mathbf{x}}_{[k|k]}$ does not depend on the actual forces $\mathbf{p}_{[k]}$. The gain matrices depend on the noise covariance matrices $\mathbf{Q}$, $\mathbf{R}$, and $\mathbf{S}$, on the forces to be estimated, as well as on the sensor configuration.

In the equations above, the system is assumed to be time-invariant. The algorithm can, however, be readily extended to time-variant systems by replacing the system matrices **A**, **B**, **G**, and **J**, with the system matrices $\mathbf{A}_{[k]}$, $\mathbf{B}_{[k]}$, $\mathbf{G}_{[k]}$, and $\mathbf{J}_{[k]}$, that depend on the time step k.

After applying the joint input-state estimation algorithm, the estimated state vector $\hat{\mathbf{x}}_{[k|k]}$ and force vector $\hat{\mathbf{p}}_{[k|k]}$ can be used to estimate the output at any location in the structure, using the following modified output equation:

$$\hat{\mathbf{d}}_{\mathrm{e}[k|k]} = \mathbf{G}_{\mathrm{e}}\hat{\mathbf{x}}_{[k|k]} + \mathbf{J}_{\mathrm{e}}\hat{\mathbf{p}}_{[k|k]} \tag{7}$$

where $\hat{\mathbf{d}}_{\mathrm{e}[k|k]}$ is the estimated response. The matrices $\mathbf{G}_{\mathrm{e}}$ and $\mathbf{J}_{\mathrm{e}}$ correspond to the extrapolated output quantities $\hat{\mathbf{d}}_{\mathrm{e}[k|k]}$ and are therefore different from the original matrices **G** and **J** in equation (2).

Very often unknown forces such as wind loads are acting on the structure. For these loads, the force locations or spatial distributions are not well known. In this case, the estimated forces $\mathbf{p}_{[k]}$ compensate for any unknown source of vibration and an attempt is made to identify equivalent forces instead of the true forces acting on the structure [9].

3. MEASUREMENT SETUP

The structure under consideration in this paper is a footbridge, located in Ninove (Belgium) [16]. The two-span cable-stayed steel bridge, shown in figure 1, has a main and secondary span of 36 m and 22.5 m, respectively. The experiments on the footbridge as well as the numerical model of the structure have been discussed in [11]. A brief overview of the experiments and the model are presented here, for reference in the following.

Figure 1 : The footbridge in Ninove, Belgium.

Three different types of excitation have been considered in the experiments: (1) ambient excitation, mainly consisting of wind loads, (2) excitation by hammer impacts, and (3) excitation by pneumatic actuators developed by the Acoustics and Vibration Research Group of the Vrije Universiteit Brussel [17]. The experiments with hammer excitation are considered for force identification in section 5. The experiments with ambient excitation are considered for response estimation in section 6. Figure 2 shows the sensor configuration. The acceleration response of the footbridge has been recorded in three orthogonal directions at 12 locations on the bridge deck, using 12 wireless GeoSIG GMS-18 units. In addition, a National Instruments (NI) data acquisition system has been used to record (1) the vertical acceleration at nodes 27 and 48, obtained from PCB 393B04 uniaxial accelerometers, (2) the vertical displacement of the bridge deck at nodes 27 and 40, obtained from AWLG 008M optical displacement sensors, (3) the impact loads applied vertically at nodes 27 and 48 using PCB 086D50 instrumented hammers (mass 5.5 kg), and (4) the tension forces applied vertically by the pneumatic actuators using a PCB 222B load cell and a BD 5 load cell.

A sampling frequency of 200 Hz and 1000 Hz is used for the GMS-18 units and the NI system, respectively. The GMS-18 acceleration data and the measurement data obtained from the NI system are synchronized by maximizing the correlation between the acceleration obtained from the GMS-18

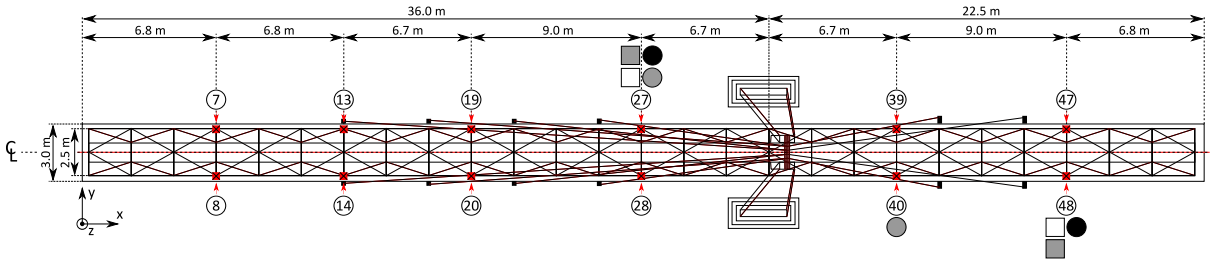

Figure 2 : Sensor configuration (white circle: GMS-18 unit, black circle: uniaxial accelerometer, gray circle: optical displacement sensor, white square: instrumented hammer, gray square: load cell).

unit at node 48 and the acceleration at node 48 obtained from the cabled uniaxial accelerometer. The measured response and force signals used in the analysis are all digitally lowpass filtered by means of an eighth-order Chebyshev type I lowpass filter with a cut-off frequency of 16 Hz, in both the forward and the reverse direction to remove all phase distortion, and then re-sampled at 40 Hz. Next, the acceleration signals obtained from the NI system and the GMS-18 units are additionally digitally highpass filtered by means of a fifth order Butterworth filter with a cut-off frequency of 0.5 Hz and 0.1 Hz, respectively, in both the forward and the reverse direction. The aim of the filter is to remove the low frequency components from the signals that are contaminated by measurement noise. Finally, a detrend operation is applied to all acceleration signals to remove the (physically meaningless) DC component. The measured displacement signals are relative to the displacement at the start of the experiment.

4. SYSTEM MODEL

The force identification and response estimation are based on a state-space description of the system, given by equations (1) and (2). The system model used in the present analysis is based on a detailed finite element (FE) model of the structure, that is composed using the FE program ANSYS. Using a model based on first principles in the joint input-state estimation procedure allows for the reconstruction of forces and response at any location in the structure. In the case where models are directly identified from experimental vibration data [18, 19], the reconstruction of forces and response is restricted to locations considered in the experiments performed for the system identification. Models based on first principles are therefore more generally applicable, and can be used for a wide range of applications, such as the identification of distributed wind loads on wind turbines or moving traffic loads on bridges. In some cases, however, a high fidelity model of the structure cannot be obtained from FE-based approaches and the use of identified dynamic models is advisable. This is for example the case when drawings of the structure are not available or when the structure is too complex to accurately model by means of FE-based approaches.

In this case, an initial FE model is based on blueprints of the structure. Next, the model is calibrated using a set of experimental modal parameters that have been obtained through operational modal analysis (OMA) [18, 19]. The model calibration results in a better representation of the dynamic behavior of the structure and, therefore, increases the accuracy of model-based numerical predictions. The calibration parameters considered in this analysis are (1) the stiffnesses of the neoprene bearings, (2) the Young's modulus of the bridge deck, (3) the Young's modulus of the pylons, and (4) the effective Young's modulus of the cables. The natural frequencies and mode shapes corresponding to 14 identified modes are used as the observed quantities in the calibration procedure, i.e. modes 1 – 5, 7 – 9, 11 – 13, and 15 – 17, listed in table 1. The remaining modes, i.e. modes 6, 10, 14, and 18, are used for cross validation of the model after calibration.

Figure 3 shows modes 1, 3, and 7 obtained from the calibrated FE model. Table 1 shows the modal characteristics obtained from the FE model after calibration and a comparison to the corresponding observed quantities. The relative error on the natural frequency ε_j for mode j is defined as $\varepsilon_j = (f_j -$

$\tilde{f}_j)/\tilde{f}_j$, where f_j is the undamped natural frequency corresponding to mode j, obtained from the FE model, and $\tilde{f}_j$ is the corresponding value obtained from the system identification. In general very high MAC-values (MAC ≥ 0.89) are obtained, both for the modes included in the model calibration and the modes used for cross validation. This indicates a good overall agreement between the identified dynamic behavior of the footbridge and the one predicted by model.

A reduced-order discrete-time state-space model is constructed from the modal characteristics of the structure. The model includes all bending modes of the bridge deck with a natural frequency that falls within the frequency range 0 Hz to 20 Hz, i.e. the 18 modes listed in table 1. For each mode, the mass normalized mode shape of the FE model is used. The natural frequency and modal damping ratio are taken as the experimentally identified values. A zero order hold assumption is applied on the input vector $\mathbf{p}_{[k]}$ in the time discretization, using a sampling frequency of 40 Hz. The reader is referred to [10] for the expression of the system matrices **A**, **B**, **G**, and **J**.

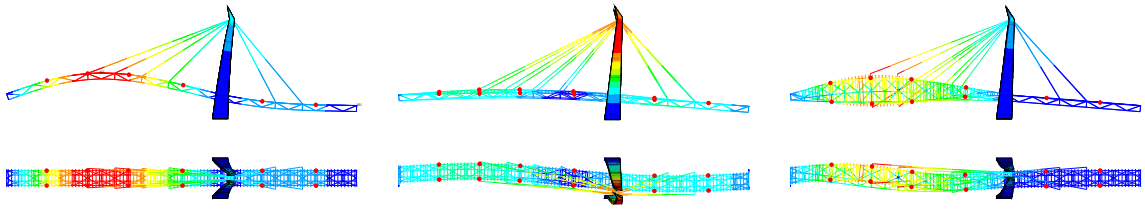

Figure 3 : Mode shape mode 1 (left), mode 3 (middle), and mode 7 (right) obtained from the calibrated FE model (top: side view, bottom: top view). The measurement locations are indicated by red dots.

j	$\tilde{f}_j$ [Hz]	$\tilde{\xi}_j$ [%]	j_{fem}	f_j [Hz]	ε_j [%]	MAC [-]	Description
1	2.93	1.16	2	3.07	4.70	1.00	1st lateral bending main span
2	2.97	0.39	1	2.87	-3.64	1.00	1st vertical bending main span
3	3.81	0.77	3	3.73	-2.11	0.99	1st combined lateral bending
4	5.79	1.04	4	5.50	-4.98	0.89	1st lateral bending secondary span
5	6.00	0.52	5	5.81	-3.09	0.98	1st vertical bending secondary span
6†	7.06	0.20	7	7.07	0.08	0.94	1st torsional main span
7	7.27	1.26	6	6.84	-5.95	0.96	2nd lateral bending main span
8	8.02	0.56	8	7.62	-5.00	0.99	2nd vertical bending main span
9	9.83	0.73	11	9.97	1.38	0.94	2nd combined lateral bending
10†	11.06	1.28	12	10.80	-2.39	0.96	1st torsional secondary span
11	11.44	2.09	13	11.60	1.38	0.94	2nd torsional main span
12	12.57	1.40	14	12.92	2.72	0.97	3rd combined lateral bending
13	13.59	0.41	15	13.07	-3.85	0.98	3rd vertical bending main span
14†	14.08	0.47	16	14.07	-0.12	0.93	3rd lateral bending main span
15	14.72	0.34	17	14.18	-3.68	0.98	2nd vertical bending secondary span
16	16.20	0.94	19	16.84	3.98	0.97	4th lateral bending main span
17	17.55	1.33	21	18.71	6.61	0.90	2nd torsional secondary span
18†	18.63	0.68	20	17.86	-4.17	0.93	4th vertical bending main span

Table 1 : Comparison between the experimentally identified modal characteristics and the modal characteristics calculated from the calibrated FE model (j: No. identified mode, $\tilde{f}_j$: identified undamped natural frequency, $\tilde{\xi}_j$: identified modal damping ratio, j_{fem}: No. corresponding mode calibrated FE model, f_j: undamped natural frequency FE model, ε_j: relative error f_j w.r.t. $\tilde{f}_j$, MAC: MAC-value). The identified modes indicated with a dagger are not included in the calibration, but used for cross validation.

5. FORCE IDENTIFICATION

This section gives a summary of the results presented in [11], where the joint input-state estimation algorithm is applied for the identification of multiple forces applied to the bridge deck of the Ninove footbridge.

Two vertical forces corresponding to hammer impacts applied at nodes 27 and 48 are estimated using a data set consisting of two vertical displacements (nodes 27 and 40) and two vertical accelerations that are collocated with the applied forces (nodes 27 and 48). The sensor configuration is determined such that (1) the conditions for instantaneous system inversion presented in [15] are met, and (2) the uncertainty on the force estimates introduced by measurement noise and wind loads is (sufficiently) small [10]. Quantification of the uncertainty requires the power spectral density (PSD) of the unknown stochastic excitation, that has been obtained from the response of the structure under ambient loading. The noise covariance matrices $\mathbf{Q}$, $\mathbf{R}$, and $\mathbf{S}$ used for joint input-state estimation are based on the PSD of the unknown stochastic excitation and the noise characteristics of the sensors [11]. The initial state estimate vector $\mathbf{x}_{[0|-1]}$ and its error covariance matrix $\mathbf{P}_{[0|-1]}$ are both assumed zero.

Figure 4 shows the results of the force identification. Firstly, a fairly good estimate of both forces is seen from both the time history and the frequency content. Three time intervals can be distinguished in figures 4b and 4e for a single hammer impact applied to the bridge deck; (1) the impact, (2) free vibration, and (3) ambient vibration. During the impact, the broad band hammer force excites the entire frequency range considered. The errors introduced by ambient forces (i.e. unknown stochastic forces) are small, since the hammer impact is far more important than the ambient loading. During the free vibration phase, the structure vibrates at its natural frequencies and modeling errors result in errors on the estimated force time history that generally decay exponentially over time. After the free vibration phase, the measured response is predominantly due to ambient loads. The ambient vibration phase is for example seen in figures 4b and 4e for $t < 104$ s. During this phase, the errors on the estimated forces originate from ambient excitation and measurement noise. The force levels observed during this phase (i.e. the force error levels) are small. It is concluded that the errors introduced by ambient excitation and measurement noise are small compared to the peak values generated by the impact forces. From the time history of the forces in figures 4b and 4e it is also seen that in this case of broadband excitation, the algorithm is able to properly distinguish between the two forces.

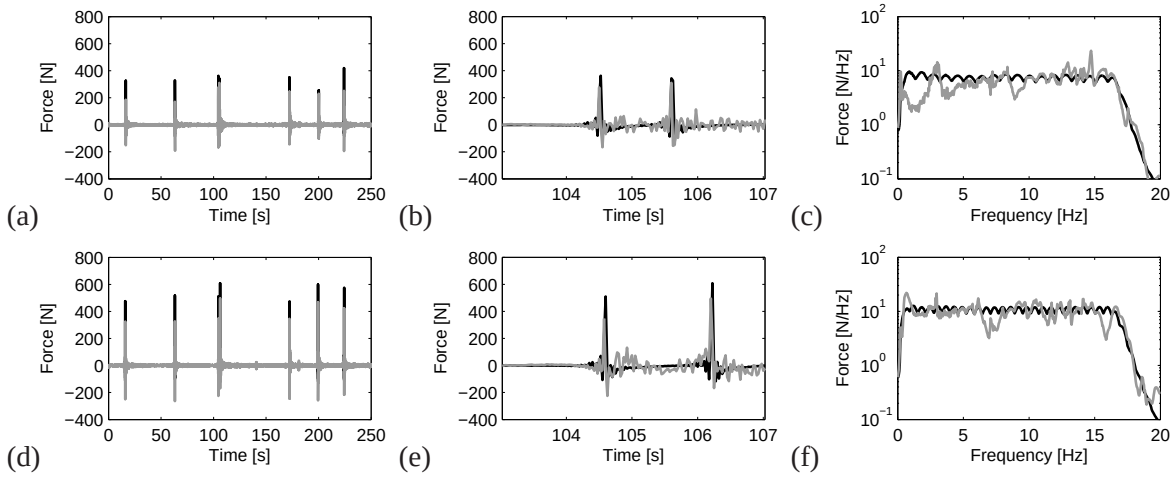

Figure 4 : Time history (left), detail of the time history (middle), and averaged amplitude of the narrow band frequency spectrum (right) of the hammer forces applied at node 27 ((a) – (c)) and node 48 ((d) – (f)). The measured force signals are shown in black, the identified force signals are shown in gray.

6. RESPONSE ESTIMATION

In this section, the lateral (y) and vertical (z) acceleration response of the bridge deck at node 7 is estimated based on eight measured accelerations: i.e. the lateral and vertical acceleration at nodes 13, 20, 27, and 48. The force vector $\mathbf{p}_{[k]}$ assumed for joint input-state estimation consists eight (equivalent) forces, that are collocated with the eight measured accelerations. Both vertical and lateral forces are assumed, as the wind loads act in both directions as well. The equivalent forces are distributed along the bridge deck, in order to be able to excite the different modes of the bridge deck. For the stability of the joint input-state estimation algorithm and the uniqueness of the estimated quantities, at least n_p displacement or strain measurements are required in addition to the measured accelerations ($n_\mathrm{p} = 8$). In this case, only two (vertical) displacements have been measured, which is insufficient. A set of displacements is therefore calculated by (offline) numerical integration of the measured accelerations. The displacements obtained by integration have been highpass filtered applying a cutoff frequency of 0.2 Hz. The aim of the filter is to remove the low frequency components from the signals which are contaminated by measurement noise. The lateral and vertical displacements at nodes 13, 20, 27, and 48 (eight displacements in total) are included in the response vector $\mathbf{d}_{[k]}$. The noise covariance matrices $\mathbf{Q}$ and $\mathbf{S}$ are chosen to be zero as the equivalent forces $\mathbf{p}_{[k]}$ are assumed to account for all excitation present. The noise covariance matrix $\mathbf{R}$ in this case accounts for sensor noise and is constructed from the (known) standard deviation of the measurement noise [11]. A standard deviation of 7×10^{-5} m/s^2 is assumed for the error on the acceleration measurements obtained from the GMS-units, that are used in the analysis. A standard deviation of 6×10^{-5} m is assumed for the error on the displacement signals that have been obtained by integration. Furthermore, the initial state estimate vector $\mathbf{x}_{[0|-1]}$ and its error covariance matrix $\mathbf{P}_{[0|-1]}$ are both assumed zero.

Figure 5 shows the results of the response estimation. A very good overall agreement between the measured and estimated accelerations is observed. The remaining errors on the estimated response mainly originate from modeling errors, which cannot be entirely avoided [11]. It is concluded that the equivalent forces succeed in accurately representing all sources of excitation acting on the structure, resulting in accurate acceleration estimates. Alternatively, the algorithm can be used to predict any response quantity of interest in the structure (see also [12]).

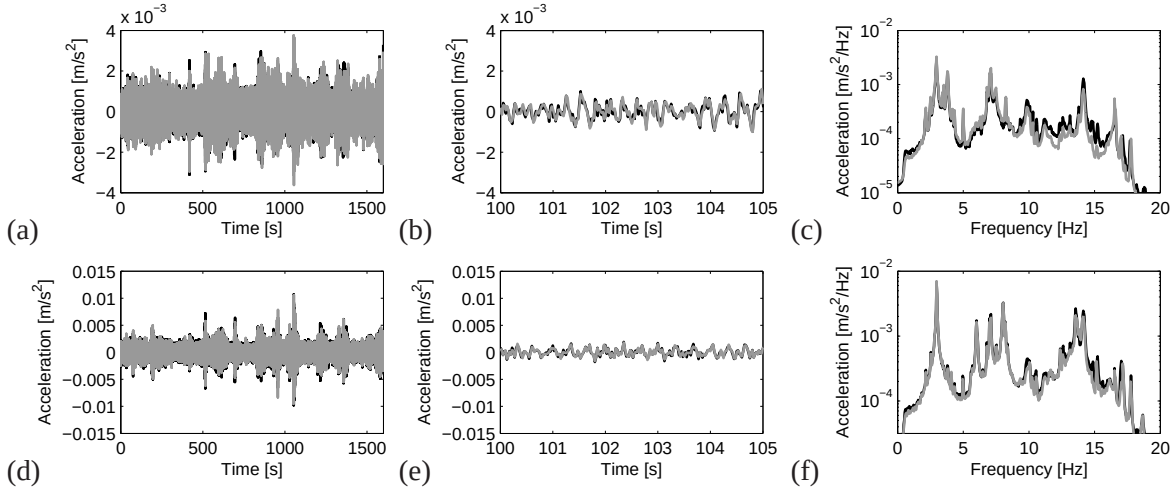

Figure 5 : Time history (left), detail of the time history (middle), and averaged amplitude of the narrow band frequency spectrum (right) of the lateral ((a) – (c)) and vertical ((d) – (f)) acceleration at node 7. The measured accelerations are shown in black, the estimated accelerations are shown in gray.

7. CONCLUSIONS

In this paper, a state-of-the-art joint input-state estimation algorithm is applied for force identification and response estimation, using data obtained from a full-scale experiment of a footbridge. First, the algorithm is used to identify two impact forces that are applied to the bridge deck. The estimated forces are in good agreement with the actual, measured forces. Some errors remain, which mainly originate from modeling errors. Second, the joint input-state estimation algorithm is used to extrapolate a set of measured accelerations to another location on the bridge deck. Comparison to the actual, measured accelerations reveals a very high estimation accuracy. These results, together with the results presented in [12], where the same algorithm is applied for the estimation of strains in the tower of an offshore monopile wind turbine, show that the algorithm can be successfully applied for response estimation, with possible applications in structural health monitoring.

ACKNOWLEDGEMENTS

The research presented in this paper has been performed within the framework of the project G.0738.11 “Inverse identification of wind loads on structures”, funded by the Research Foundation Flanders (FWO), Belgium. The authors are all members of the KU Leuven - BOF PFV/10/002 OPTEC - Optimization in Engineering Center. The financial support of FWO and KU Leuven is gratefully acknowledged.

REFERENCES

[1] D. Bernal and A. Ussia. Sequential deconvolution input reconstruction. *Mechanical Systems and Signal Processing*, 50–51:41–55, 2015.

[2] M. Klinkov and C.-P. Fritzen. An updated comparison of the force reconstruction methods. *Key Engineering Materials*, 347:461–466, 2007.

[3] Y. Liu and W.S. Shepard. Dynamic force identification based on enhanced least squares and total least squares schemes in the frequency domain. *Journal of Sound and Vibration*, 282:37–60, 2005.

[4] E.M. Hernandez. A natural observer for optimal state estimation in second order linear structural systems. *Mechanical Systems and Signal Processing*, 25(8):2938–2947, 2011.

[5] C. Papadimitriou, C.-P. Fritzen, P. Kraemer, and E. Ntotsios. Fatigue predictions in entire body of metallic structures from a limited number of vibration sensors using Kalman filtering. *Structural Control and Health Monitoring*, 18:554–573, 2011.

[6] S. Eftekhar Azam, C. Papadimitriou, and E. Chatzi. A dual Kalman filter approach for state estimation via output-only acceleration measurements. *Mechanical Systems and Signal Processing*, 60–61:866–886, 2015.

[7] Y. Niu, M. Klinkov, and C.-P. Fritzen. Online force reconstruction using an unknown-input Kalman filter approach. In *Proceedings of the 8th International Conference on Structural Dynamics, EURODYN 2011*, pages 2569–2576, Leuven, Belgium, 2011.

[8] S. Gillijns and B. De Moor. Unbiased minimum-variance input and state estimation for linear discrete-time systems with direct feedthrough. *Automatica*, 43(5):934–937, 2007.

[9] E. Lourens, C. Papadimitriou, S. Gillijns, E. Reynders, G. De Roeck, and G. Lombaert. Joint input-response estimation for structural systems based on reduced-order models and vibration data from a limited number of sensors. *Mechanical Systems and Signal Processing*, 29:310–327, 2012.

[10] K. Maes, A.W. Smyth, G. De Roeck, and G. Lombaert. Joint input-state estimation in structural dynamics. *Mechanical Systems and Signal Processing*, 70–71:445–466, 2016.

[11] K. Maes, K. Van Nimmen, E. Lourens, A. Rezayat, P. Guillaume, G. De Roeck, and G. Lombaert. Verification of joint input-state estimation for force identification by means of in situ measurements on a footbridge. *Mechanical Systems and Signal Processing*, 75:245–260, 2016.

[12] K. Maes, A. Iliopoulos, W. Weijtjens, C. Devriendt, and G. Lombaert. Dynamic strain estimation for fatigue assessment of an offshore monopile wind turbine using filtering and modal expansion algorithms. *Mechanical Systems and Signal Processing*, 76–77:592–611, 2016.

[13] R.E. Kalman. On the general theory of control systems. In *Proceedings of the First International*

Congress of IFAC, Moscow, 1960.

[14] H.P. Hjelm, R. Brincker, J. Graugaard-Jensen, and K. Munch. Determination of stress histories in structures by natural input modal analysis. In *Proceedings of IMAC XXIII International Modal Analysis Conference*, pages 838–844, Houston, Texas, 2006.

[15] K. Maes, E. Lourens, K. Van Nimmen, E. Reynders, G. De Roeck, and G. Lombaert. Design of sensor networks for instantaneous inversion of modally reduced order models in structural dynamics. *Mechanical Systems and Signal Processing*, 52–53:628–644, 2015.

[16] K. Van Nimmen, G. Lombaert, G. De Roeck, and P. Van den Broeck. Vibration serviceability of footbridges: Evaluation of the current codes of practice. *Engineering Structures*, 59:448–461, 2014.

[17] K. Deckers, P. Guillaume, D. Lefeber, G. De Roeck, and E. Reynders. Modal testing of bridges using low-weight pneumatic artificial muscle actuators. In *Proceedings of IMAC 26, the International Modal Analysis Conference*, Orlando, FL, February 2008.

[18] E. Reynders and G. De Roeck. Reference-based combined deterministic-stochastic subspace identification for experimental and operational modal analysis. *Mechanical Systems and Signal Processing*, 22(3):617–637, 2008.

[19] B. Peeters and G. De Roeck. Reference-based stochastic subspace identification for output-only modal analysis. *Mechanical Systems and Signal Processing*, 13(6):855–878, 1999.